PAPER Nr. 25

COMPREHENSIVE AERODYNAMIC RESERRCH INVOLVED IN MI-38 DEVELOPMENT

BY

A.N.IVANOV, M.G.ROZHDESTVENSKY,
A.P.VAINTRUB AND V.A.IVCHIN

MIL MOSCOW HELICOPTER PLANT
MOSCOW,RUSSIA

TWENTIETH EUROPEAN ROTORCRAFT FORUM
OCTOBER 4 - 7, 1994 AMSTERDAM

Printed by the Technical Highschool Haarlem

COMPREHENSIVE AERODYNAMIC RESEARCH INVOLVED IN MI-38 DEVELOPMENT

A.N. Ivanov,
Chief Designer
M.G. Rozhdestvensky,
Head of Department
A.P. Vaintrub,
Team Leader
V.A. Ivchin,
Team Leader
Mil Moscow Helicopter Plant,
Russia

SUMMARY

The paper is dedicated to development of the Mi-38 medium-lift helicopter. Comprehensive experimental research done to support design efforts, as well as the philosophy used to solve the basic aerodynamic problems of the Mi-38 are highlighted.

Features inherent in the main and tail rotor blade aerodynamic layout are considered, data obtained from flight tests and experimental research and used as the basis for choosing the blade aerodynamic configuration as well as the leading particulars of airfoils providing high lift capability of the main rotor at relavely low levels of the blade pitch moments are analysed.

Great attention is paid to comprehensive studies involved in the definition of the airframe streamlined shape as well as to minimization of the main and tail rotor hub drag. The effect of layout and design solutions on the airframe drag and moment characteristics is shown.

The experiment carried out to obtain the main rotor performance at low velocities corresponding to advance ratio values (μ) ranging from 0 to 0.10 and the rotor downwash influence on the horizontal stabilizer in these flight conditions are described. As a result of these experiments, specific features inherent in variation of the main rotor performance at low velocities have been found; these features have allowed us to acquire a new insight into the causes of nonlinear variation of the helicopter trim characteristic in the longitudinal plane at low airspeeds.

LIST OF SYMBOLS

C_T	rotor thrust coefficient
σ	rotor solidity
M	Mach number
η_0	hover figure of merit
δ, deg	blade tip anhedral angle
C_{lmax}	maximum airfoil lift coefficient at 0.4M
$M_{dd/Cl=0}$	drag divergence Mach number at $C_l = 0$
$K_{max}=L/D$	airfoil maximum L/D ratio
m_{zo}	airfoil pitch moment relative to airfoil nose
$\overline{V}$	relative airflow velocity
α, deg	rotor angle of attack
Y	normal force produced by horizontal stabilizer
$K=L/D_e$	aircraft L/D ratio where
L	lift
D_e	eqiuvalent drag with due account of power losses for driving main rotor
N_{lf},shp	level flight power required
h, m	flight altitude
V_y, m/s	vertical component of airspeed
n ,%	main rotor speed, MR 95% corresponds to main rotor tip speed of 215 m/s
N, shp	powerplant power
φ,deg	main rotor collective pitch
υ,deg	helicopter pitch
V_x km/h	horizontal component of airspeed

1 INTRODUCTION

The Mi-38 helicopter under development is to replace the Mi-8, the world's well known and popular helicopter, and its modifications which together make up a family in the medium category well proven during more than 25 years of their operation.

The Mi-38 high power-weight ratio and advanced aerodynamic layout of the main rotor blade allow us to be confident in obtaining high performance within wide altitude and temperature ranges.

Table 1 shows leading particulars of the helicopter for ISA and SL conditions.

Table 1

Takeoff weight,kgf	**normal 14,200**	**maximum 15,500**
Hovering ceiling, OGE, m	2,600	1,300
Service ceiling, m	5,200	4,200
Cruise speed km/h	275	265
Maximum speed km/h	295	285

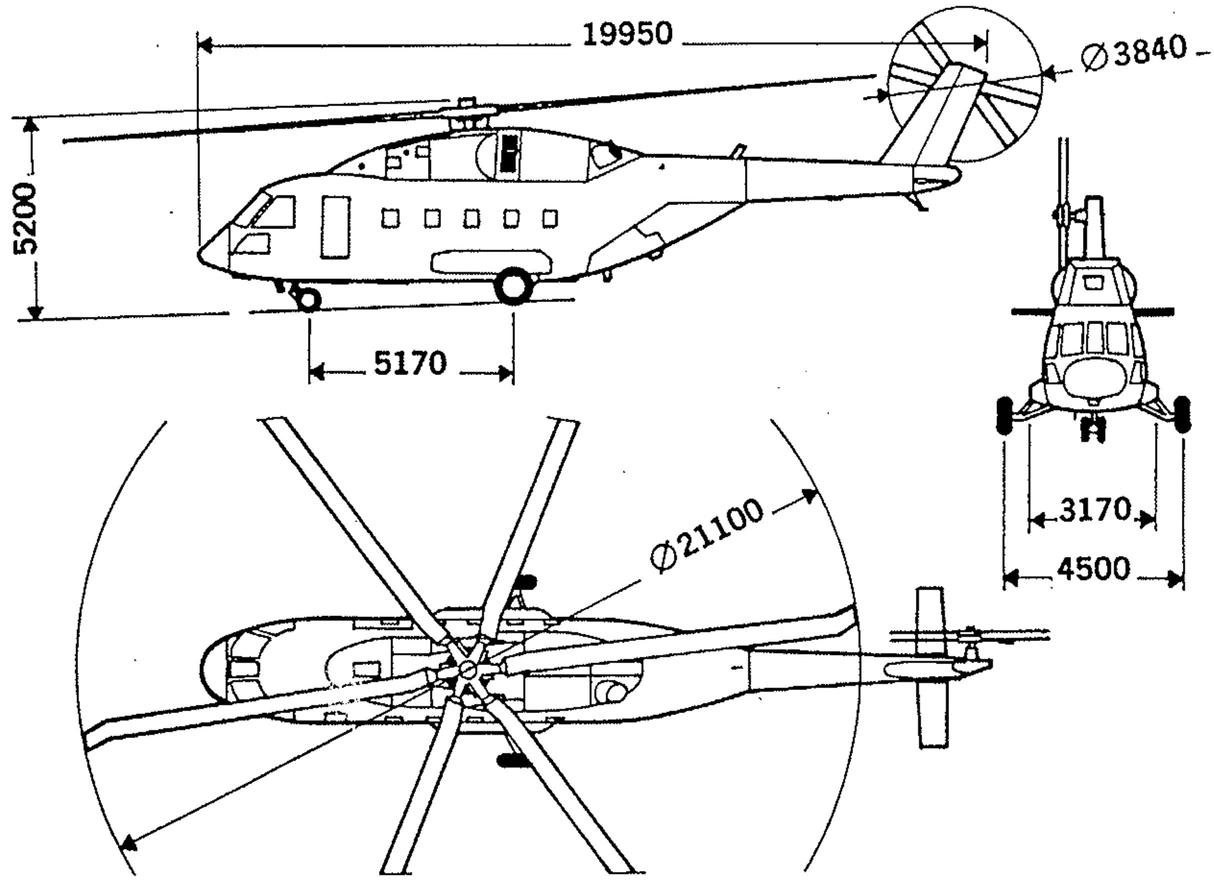

Fig.1. MI-38 three view drawing

2 MAIN ROTOR BLADE AERODYNAMIC LAYOUT FEATURES

The 21.1-meter diameter main rotor has 6 blades of rectangular planform incorporating sweptback tips. The blade tip starting at spanwise station 0.95R has a 30 deg. sweep at the leading edge and a 15 deg. sweep at the trailing edge. This tip shape choice was based on the flight test results obtained for the Mi-28 blade prototypes having sweptback tips. The tests confirmed the efficiency of sweptback tips as a means to reduce the constant of the swashplate moment. In level flight at maximum speeds the loads were reduced by 20%, and in maneuvering, up to 25%.

The blade twist chosen was a compromise to obtain the main rotor hover figure of merit as high as possible along with an acceptable level of varying stress in the blade spar at maximum airspeeds. The middle portion of the blade has a twist corresponding to 12.5 deg. per radius while the blade root up to 0.1R has no twist at all due to design considerations.

To improve the main rotor efficiency, research was done to define the effect of the tip having anhedral geometry on main rotor hover performance. A 3.5-meter diameter main rotor model having three versions of blades (i.e. blades with straight tips and tips of anhedral geometry bent down flatwise at 7 and 14 degrees respectively) has been tested on the whirl tower designed for investingating scale main and tail rotor performance in hover. The tip started at 0.95R. From the rotor polars obtained, the effect of the tip anhedral geometry on the rotor hover figure of merit has been determined. Diagrams in Fig. 2 show the improvement of the figure of merit of the main rotor having blade tips of anhedral geometry over that of the rotor

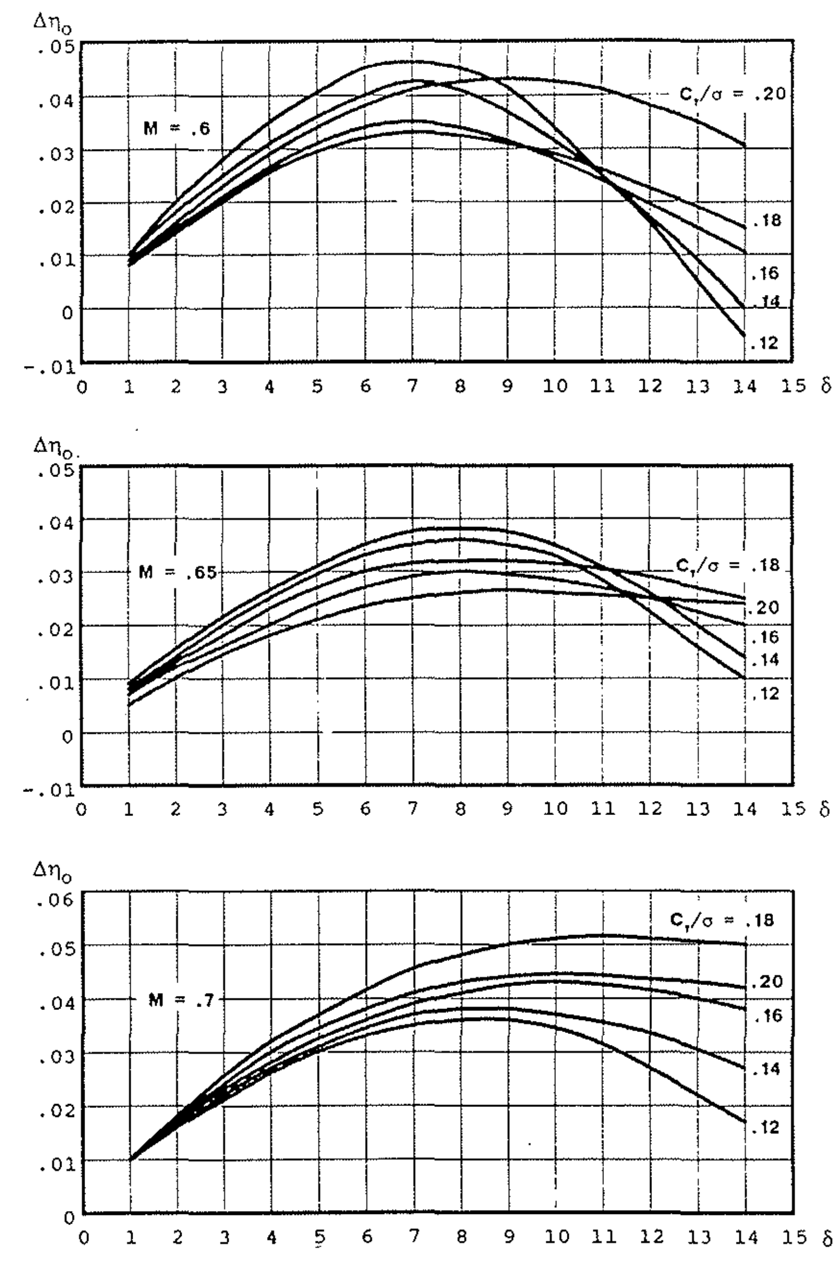

Fig.2. Influence of MR blade unheadral hover figure of merit increment.

with the straight blade tips for different values of the thrust coefficient and two tip Mach numbers.

As can be seen from the presented results, the anhedral geometry in the Mach number range corresponding to the full-scale blade tip speed leads to an increase of the hover figure of merit by 3-4%.

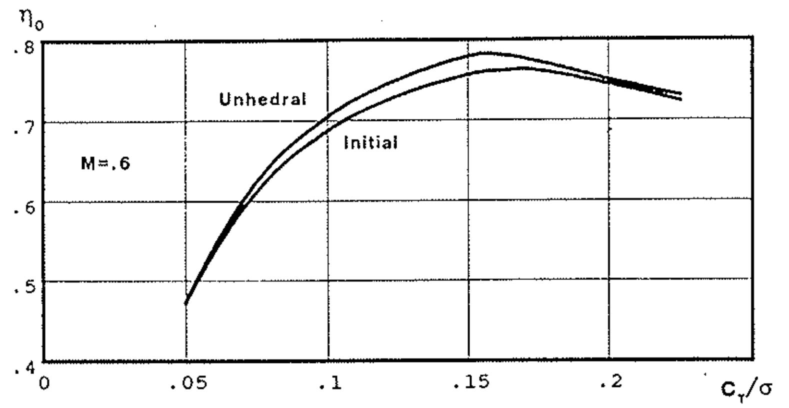

Fig.3. Influence of MR blade unhedral on figure of merit.

It should be noted that this improvement has been obtained for the rotor whose initial figure of merit was quite high: for instance, the rotor figure of merit was 0.7 at 0.6M for the thrust coefficient ranging from 0.14 to 0.18. From the test results presented, it can be seen that as the tip Mach number increases the maximum rotor figure of merit is obtained at higher anhedral values.

The results of this research are to be used in upgrading the main rotor blades to improve the main rotor thrust performance. Fig. 3 shows hover figure of merit versus thrust coefficient curves for main rotors whose blades use the same airfoils but have different anhedral geometry at the tips. As the calculations made have shown, the anhedral angle of 7 deg. at station 0.95R will allow the Mi-38 main rotor to improve the figure of merit by 2-3% at thrust coefficients ranging from 0.14 to 0.18.

When developing rotor blade aerodynamic layout, the Mil Helicopter Plant does the job in close cooperation with the Central Aero-Hydraudynamic Institute (TsAGI). Airfoils developed in the TsAGI department headed by E.S. Vozhdaev are primarily used in the majority of the Mil helicopters showing quite a high figure of merit. The Mi-38 main rotor design also uses TsAGI airfoils developed with due account of the requirements imposed by the Customer on the helicopter in terms of its hovering ceiling and temperature range, as well as its maximum airspeeds, taking into consideration design features and manufacturing processes at the same time. High maximum and cruise speeds have required that a thin airfoil (the KCM airfoil according to the TsAGI designation) of 9% thickness ratio having a high Mach critical number should be utilized for the blade tip. This airfoil is used for the

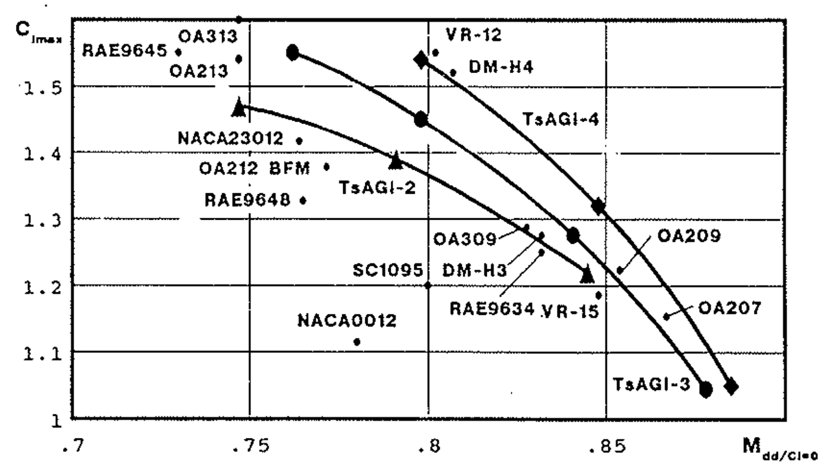

Fig.4. TsAGI airfoil characteristics in comparison with those of other airfoils.

sweptback tip. The main portion of the blade (running from station 0.3R to station 0.91R) uses the CBM airfoil which has a highlifting capability and high L/D ratio that remain the same with the change of the thickness ratio from 11% to 14%.

Fig. 4 presents points characterizing the airfoils used in main rotor blades in terms of maximum lift coefficient at 0.4M as well as in terms of critical Mach number at zero airfoil lift. The characteristics of these airfoils have been obtained in the same TSaGI wind tunnel, thus the presented comparison is quite rightful.

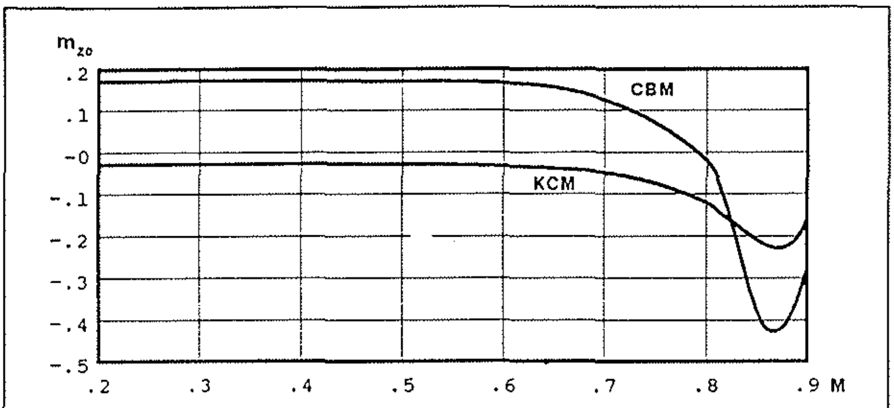

Fig.6. Airfoil pitch moment coefficient vs Mach number.

In the same figure connected are the points characterizing the airfoils of three TsAGI series developed during the recent years. For the Mi-38 main rotor blades, the airfoils of the third series which had been developed by the time the helicopter was conceived are used. Fig. 5 presents the maximum L/D ratio of the airfoils used in the Mi-38 main rotor blades versus Mach number. A more advanced series of the TSaGI-4 airfoils has been recently developed and they are expected to be used in the latest version of the Mi-28 Army helicopter, and quite probably, in the subsequent upgrading of the Mi-38 main rotor.

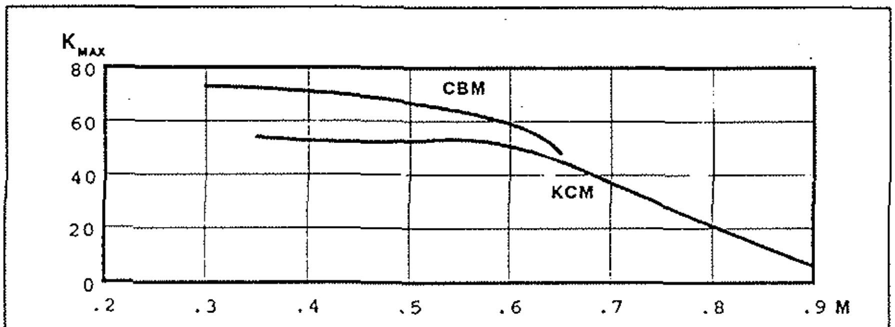

Fig.5. TsAGI-3 maximum L/D ratio vs Mach number.

One of the main benefits of the airfoils utilized is an insignificant change in the value of the airfoil pitch moment coefficient (m_{zo}) with Mach number. As can be seen from the diagram in Fig. 6, the pitch moment coefficient of the KCM airfoil is negative within the whole range of Mach numbers remaining practically constant up to 0.7M and having a small spoon-shaped dip in the nose down pitch for 0.8M to 0.9M.

The pitch moment coefficient change with Mach number is also quite favourable for the CBM airfoil, especially, if its spanwise position is taken into account. The maximum value of Mach number obtained on the advancing blade CBM airfoil does not exceed 0.8M and, as can be seen from the diagram, the coefficient m_{zo} in flight at maximum airspeeds changes by not more than 0.02. These airfoil characteristics allow us to expect a relatively low level of loads applied to the swashplate.

3 AIRFRAME DRAG MINIMIZATION

Refinement of the helicopter airframe shape was the main objective of the Mi-38 scale model wind tunnel tests conducted in the TsAGI; drag and moment characteristics of the airframe were determined during these tests. It should be pointed out, that, at the design stage, meticulous analysis of the research work and flight test results of the Mi-8 connected with airframe drag minimization was made. The results of this work were presented by A.I.Akimov [1] at the 19th European Rotorcraft Forum.

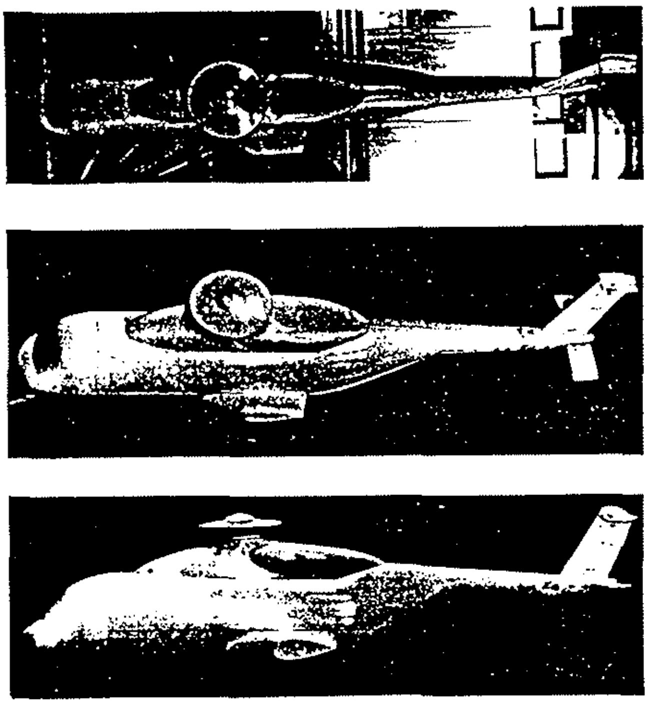

Fig.7. One of the MI-38 wind-tunnel model versions

To make principal decisions during the helicopter development that will define its external appearance, three stages of the scale model wind testing had to be conducted. They were carried out to refine the airframe shape to minimize its drag and to determine the interference created by the airframe components such as the LG sponsons and the horizontal stabilizer.

Fig. 7 shows a photo of one of the scale model versions tested in the wind tunnel. During these wind tunnel tests some features of the airflow around the nose section of the airframe, as well as around the main gearbox and engine cowls were revealed. These features are visualized by using the oil film method. The whole helicopter scale model is covered with a black oil film. The black film covering the surfaces where the airflow moves smoothly is blown off and the model acquires the original white colour. The surfaces of the model airframe remained black show some negligible airflow velocity over them which, as a rule, is a result of the airflow separation. One of the photographs obtained during the tests is shown in Fig. 8 where figures 1, 2 and 3 indicate stagnation areas and airflow separation from the surface. Proceeding from the wind tunnel test results, the configuration of the airframe nose section was modified leading to a reduction in the airframe drag by 15%.

In Fig.9 solid lines show the final version of the Mi-38 wind tunnel scale model which was obtained after several modifications aimed to minimize the airframe drag and improve its moment characteristics. Dotted lines show main versions of the wind tunnel scale model whose performance was studied in wind tunnel tests.

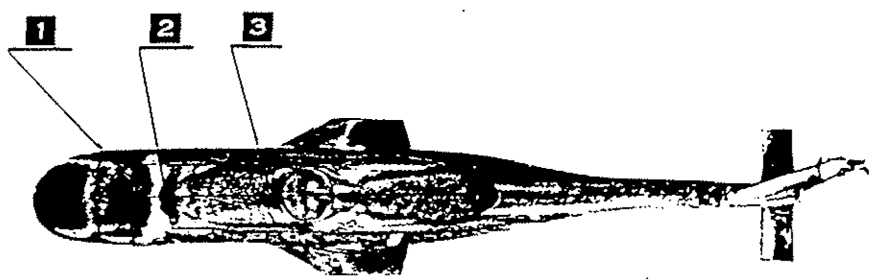

Fig.8. Foto of the MI-38 airframe model outer surface after wind tunnel testing using the oil-film method

4 OPTIMIZATION OF HORIZONTAL STABILIZER AREA AND POSITION

Quite a serious problem to be solved during the course of defining the airframe aerodynamic shape was how to provide the required static stability and what area and position of the horizontal stabilizer should be. The fact is that this greatly depends upon the shape and dimensions of the LG sponsons. The landing gear was first conceived as a retractable one with wheels to be retracted into dedicated sponsons located beyond the fuselage outline as the underfloor space was allocated for large capacity fuel tanks.

The side sponsons (Fig. 9) having a streamlined section in the shape of a wing airfoil of high thickness ratio were actually stub wings. These stub wings having relatively small profile drag produced some lift and, therefore, a wake which, impinging on the horizontal stabilizer, greatly reduced its efficiency, particularly at positive angles of attack. As a result, the stabilizer area had to be significantly increased. The calculations showed that, to achieve acceptable stability, the stabilizer should have an area of 3 sq. m but the reduced efficiency caused by the wake distorted airflow required to increase this area to 4 sq. m.

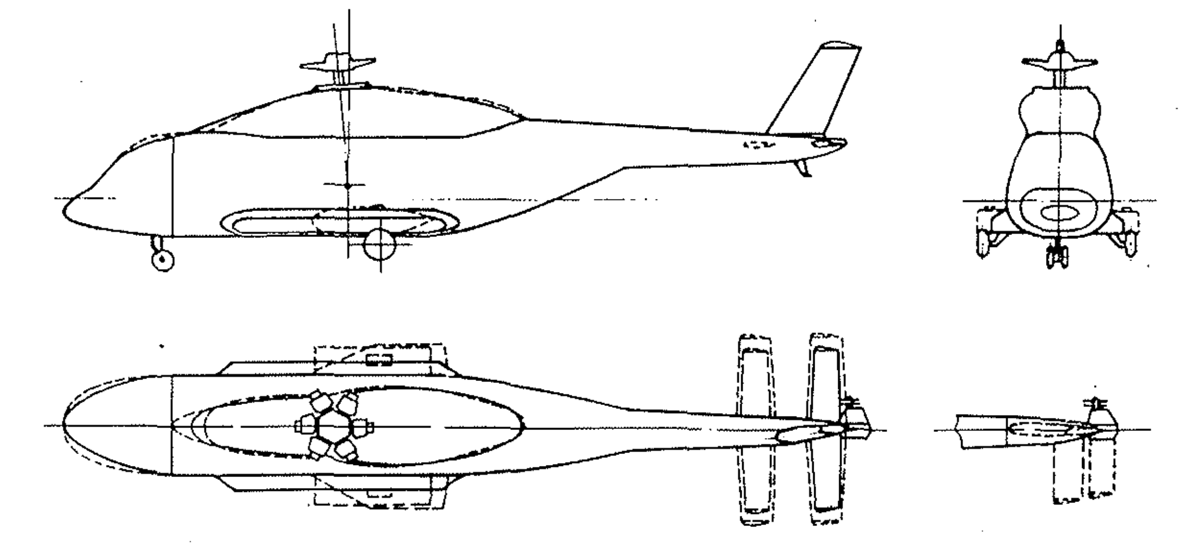

Fig.9. MI-38 wind tunnel model variants.

Design studies of a one-sided high-set stabilizer showed quite a significant increase of the tail boom weight as compared to that with a symmetrical stabilizer installed on the tail boom. Besides, the one-sided stabilizer of 2 sq.m area did not provide the required dynamic stability of the helicopter. To increase the one-sided stabilizer area up to 3 sq. m was quite problematic due to design and weight considerations. However, these problems were essentially simplified when the concept of helicopter operation had been changed. The project Customer and Operators' representatives, well aware of the conditions under which the helicopter was to operate in Western Siberia (from unpaved and unprepared sites) with a great air temperature difference and high relative humidity, and unavoidable penetration of snow, ice and mud into the LG retraction system, had expressed their great doubts about trouble-free operation of the LG retraction and extension system. Their arguments were so convincing that a decision was made to give up the retractable landing gear. This design change resulted in an increase of the helicopter drag equivalent to flat-plate drag of 0.55 sq.m but at the same time the landing gear system became much simpler, lighter in weight and more reliable.

The nonretractable landing gear allowed to give up sponsons of large volume and area that had been intended for rectracting the wheels in flight, and to use much smaller sponsons to accommodate the elements of the landing gear tubular structure attachment components protruding beyond the fuselage outline. Those who were in charge of the general arrangement were filled with joy and stuffed the free space with different equipment components immediately; you know it perfectly that accommodation of numerous equipment items within the limited space of the aircraft is always a difficult problem to solve.

Wind tunnel tests of the appropriately modified scale model showed that the airflow pattern had greatly changed in the airframe tail area and the stabilizer downwash angles had reduced. This led to a sunstantial change in static stability, particular in the value of the longitudinal moment derivative with respect to the angle of attack. If the airframe incorporating sponsons for the retractable landing gear and the stabilizer of 3 sq. m area had no longitudinal static stability, the airframe version with the nonretractable landing gear became statically stable within a wide range of angles of attack from - 14 up to + 10 deg. for the stabilizer of the same area.

5 INVESTIGATIONS OF MAIN ROTOR AND STABILIZER SCALE MODEL PERFORMANCE AT LOW AIRFLOW VELOCITIES

From the flight test results it is known that the longitudinal cyclic stick trimmed position versus airspeed curve has the so-called spoon-shaped dip at low airspeeds. This dip affects the longitudinal control and stability of the helicopter at low airspeeds. A very typical nonlinearity of the trimmed pitch angle curve occurs in the same range of low airspeeds.

The occurrence of this dip in the trim curves is usually attributed to the change in the rotor diskwise distribution of induced velocities affecting blade flapping and airflow around the airframe, the horizontal stabilizer included.

To gain a deeper insight into the physical nature of this phenomenon and the causes leading to it, as well as to determine more exactly the stabilizer position relative to the Mi-38 main rotor axis, research was done on a scale main rotor to define the rotor performance and the effect of the rotor wake on the horizontal stabilizer at airflow velocities corresponding to small advance ratio values.

Due to the fact that a stable low speed airflow cannot be obtained in any wind tunnel, tests were carried out in the TSaGI water channel whose dimensions (it is about 100 m long and 6 m wide) allowed to move the scale rotor and stabilizer placed behind it (both mounted on a special platform) in a still air at a calibrated speed. The same platform accommodated the researchers, as well as the test control system and data acquisition and processing system. Fig. 10 shows the facility on which the test was conducted. A 2.55-meter diameter 5-bladed scale rotor model whose solidity was 0.105 was subject to test. The blade tip speed was 80 m/s. The stabilizer span was 0.584 m,the mean chord being 0.085 m. During the tests the platform accommodating the above rotor and stabilizer moved at speeds from 0 to 9 m/s.

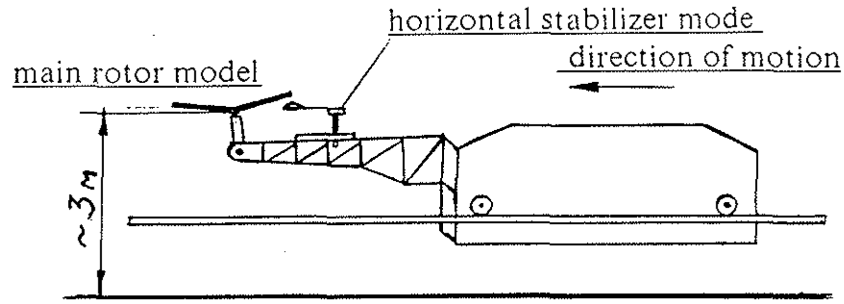

Fig.10. Main rotor and horizontal stabilizer scale models installed on the platform for testing in the TsAGI water tunnel

As a result of the tests, some peculiar changes in the rotor longitudinal force at low airflow velocities were discovered. Fig. 11 presents rotor longitudinal force coeffficient versus airflow velocity curves clearly showing a nonlinearity, i.e. a dip of the longitudinal force coefficient versus airflow velocity curve.

interest. Fig. 12 shows the results of stabilizer force measurements at three different positions relative to the main rotor. The three positions of the stabilizer differed either by the distance between the stabilizer and the main rotor axis ($\overline{X}$ = x/R = 0.9 and 1.13) with the position of the stabilizer in relation to the plane of rotation being the same

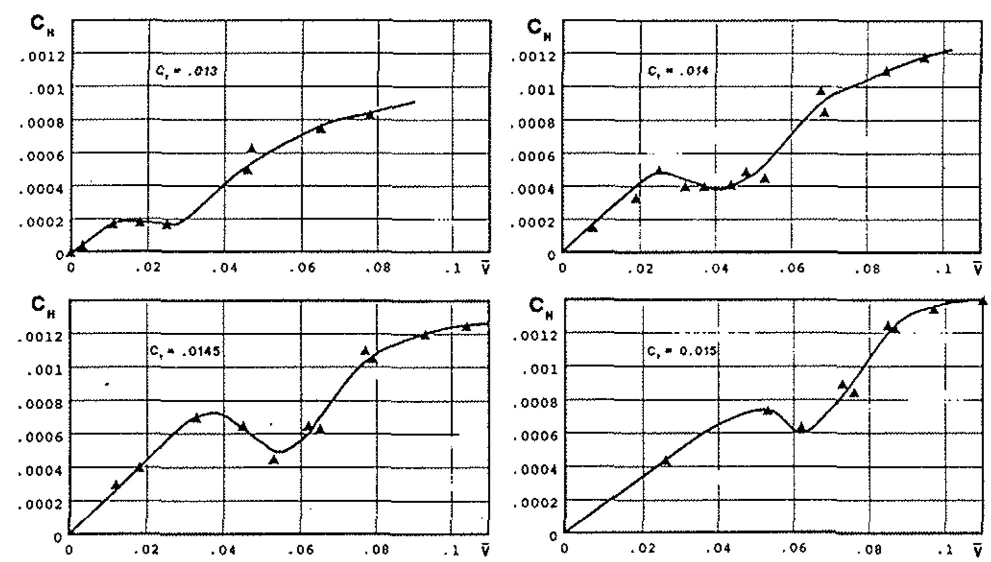

Fig.11. Main rotor longitudinal force vs airflow velocity.

($\overline{Y}$ = y/R = 0.15), or by the different distance between the stabilizer and the plane of rotation ($\overline{Y}$ = 0.15 and 0.095) with the distance to the main rotor axis being the same ($\overline{X}$ = 1.13). Fig. 12 also shows different alternatives of the stabilizer position in relation to the main rotor and stabilizer vertical force variation with airspeed for these positions. As can be seen from the

The nonlinearity of the above characteristic in the range of low airflow velocities ($\overline{V}$) was found out; it appears to be one of the causes for a change in the nature of the helicopter longitudinal trim at low airspeeds, which is the so-called spoon-shaped dip.

The results obtained during measurements of forces applied to the horizontal stabilizer were of no lesser

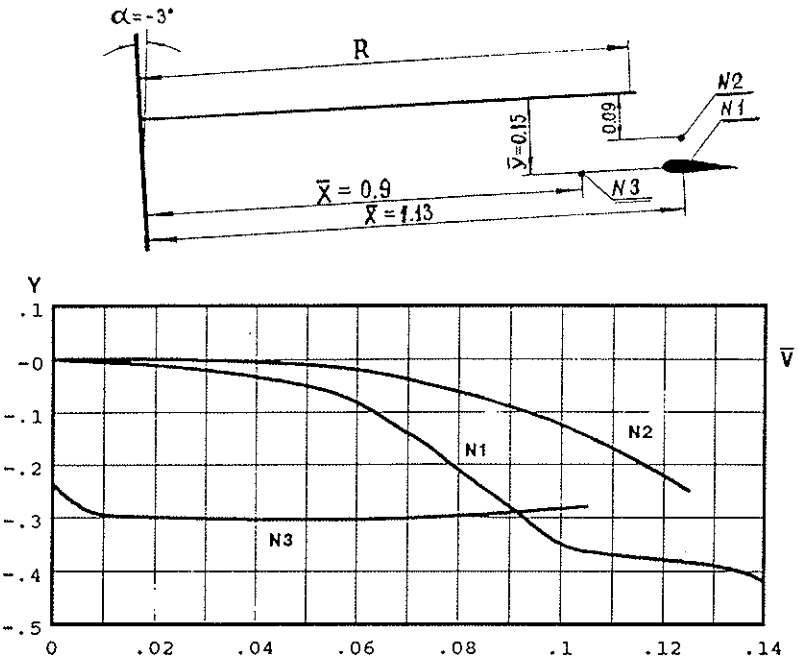

Fig. 12. Horisontal stabilizer lift vs airflow velocities for different stabilizer positions relative to MR axis.

presented data, when the stabilizer is positioned beyond the main rotor blades ($\overline{X}$= 1.13) the stabilizer force is very small at airspeeds up to $\overline{V}$=0.05, and only when this airspeed is reached, the downward force starts growing. The most intensive growth of the force with airspeed occurs on stabilizer No. 1 located at a long distance from the main rotor. For stabilizer No. 3, the stabilizer force actually remains the same within the whole range of airspeed changes $0 < \overline{V} < 0.1$ and is equal to 1% of the main rotor thrust or takeoff weight. When the stabilizer is located behind the main rotor (stabilizer No. 1) the load applied to the stabilizer reaches the same value only at $\overline{V}$ = 0.09 which allows to obtain a gain in the payload.

The way the stabilizer forces versus airspeeds curves change does not lead us to state that the moments produced by the stabilizer cause the occurrence of the spoon-shaped dip in the helicopter trimmed longitudinal control curve at low airspeeds.

Research into rotor and horizontal stabilizer scale model performance was done by our colleagues from the TSaGI, Mr. V.F. Antropov and Mr. I.O. Faktorovich

6 TAIL ROTOR AERODYNAMIC CONFIGURATION FEATURES

The tail rotor consists of two pairs of blades installed in such a way that the angle made up by these two pairs in the plane of rotation is not 90 degrees. The rotor of this configuration is called an X-shaped one, or scisssors. The smallest angle between the two pairs of the blades is 36 degrees. In addition, they have a distinctive feature in that these two pairs are installed on the tail rotor shaft at a distance so that the X-shaped rotor is made up of two pairs of two-bladed rotors located in two different levels.

This configuration has been chosen for different reasons. One of them was to increase the tail rotor hover figure of merit and, thus, to reduce the power consumed. Full-scale whirl tower tests of the experimental tail rotor made up of two pairs of two-bladed modules that can be installed at different angles relative each other in the plane of rotation have shown that the tail rotor hover figure of merit is distinctly optimal within the range of angles from 30 to 40 degrees. This result can be attributed to a reduced effect of the vortex sheet created by one pair of the blades on the other. Reduced vortex interference is also achieved by the location of two pairs of the blades in two different levels along the rotor shaft. To improve the rotor hover figure of merit, the tail rotor blades have a twist, which was used for the first time in Mil tail rotor blades.

The information obtained from foreign literature that the tail rotor of this configuration produces less noise in comparison with the rotor whose blades are installed perpendicular to each other has played a significant role in choosing this configuration of the tail rotor.

Comparative flight tests were conducted on one and the same helicopter on which a three-bladed conventional rotor and an X-shaped rotor having the same diameter, thrust and power characteristics were installed in turn. The external noise where the tail rotor noise level is the dominating one has been measured. The comparison of the measurements has shown that the X-shaped rotor noise level was by 3-5 EPNdB lower than that of the conventional tail rotor.

From the design point of view, the rotor configuration having two pairs of blades located in two different levels is quite attractive because the structural and mechanical arrangement of the head becomes much simpler as the centrifugal force produced by each blade is counteracted by that of the opposite blade, and flatwise blade flapping is ensured by rotation of the flapping hinge which is common for each pair of the blades.

The TSaGI MБ airfoil is used in the blade design featuring high values of maximum lift and figure of merit. The new airfoil application has resulted in an increase in the rotor hover figure of merit by 1.5-2.4% and a wider range of the margins of directional control as compared to those provided by the well known and widely used NACA-230-12 airfoil.

Although the X-shaped tail rotor has advantages, we are aware of the fact that the rotor head configuration adopted by us has a slightly higher drag as compared with that of the conventional head whose rotor blades are arranged in one plane only.

7 RESULTING MI-38 AERODYNAMIC EFFICIENCY

The results obtained from comprehensive studies in the field of developing an effective main rotor and refining the airframe shape can be reflected in the total helicopter L/D ratio, according to Hohenemser's statement. Fig. 13 shows helicopter L/D ratio versus airspeeds for two altitudes, i.e. SL and 2,000 m, at normal takeoff weight of 14,200 kg. The blade tip Mach number variation, besides a natural variation of the sound velocity with altitude, reflects one of the helicopter design features, i.e. to delay the main rotor blade stall at maximum airspeeds at altitudes exceeding 2,000 m, the main rotor tip speed increases from 215 m/s to 225 m/s.

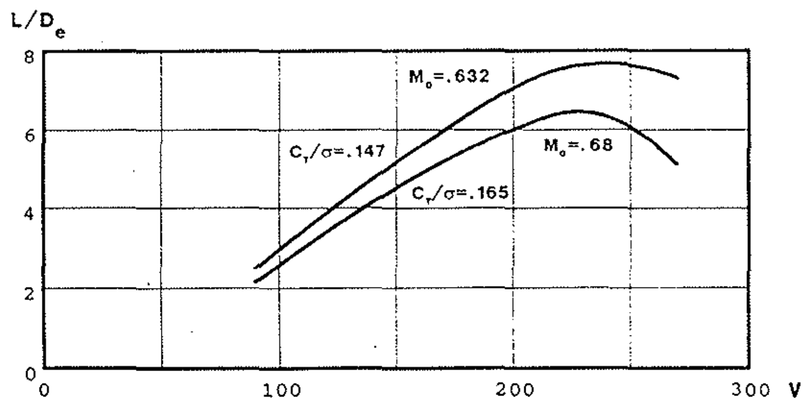

Fig.13. Mi-38 L/D ratio vs airspeed.

A significant feature differing the Mi-38 from the Mi-8 is an improved level of flight safety when one engine fails during takeoffs and landings which is ensured mainly by a high 30-second OEI power rating of the engine. This rating exceeds the takeoff power rating by 50%. It should be noted that the above stated relation existing between these two power ratings was not an inherent feature of the engine at the very start of its development. Work on engine development is being done parallel to helicopter development; it has passed a few stages, that is, when the inability of the engine to meet the helicopter design bureau requirements for high contingency power ratings was revealed, its initial arrangement and parameters were revised.

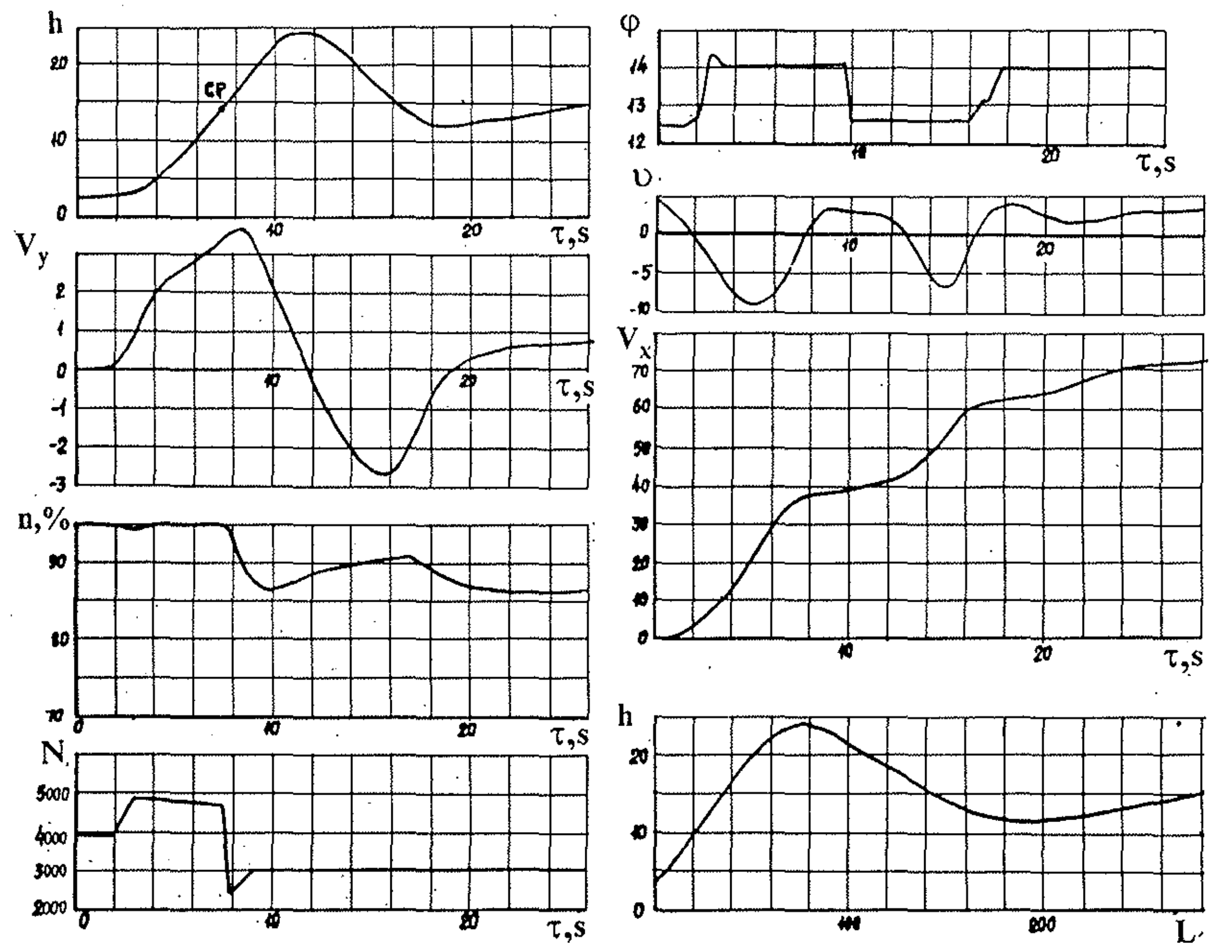

Fig.14. Helicopter motion main parameters variation in OEI continued take-off from the critical point(H=500m, ISA+5°,M=14200kg).

At the present development stage of the Mi-38, its engines have the following main power ratings in ISA:

30-second OEI power rating, 3,750 shp
2.5-minute OEI power rating, 3,600 shp
30 - minute OEI maximum continuous power rating, 2,900 shp
takeoff power rating, 2,500 shp

The above stated high OEI power ratings of the engine combined with its rapid acceleration has allowed us to ensure good takeoff and landing performance of the helicopter in Category A specified in FAR Part 29 requirements calling for a high level of flight safety at any stage of flight.

Our simulation work on the flight simulator where the mathematical model of full helicopter motion was implemented in combination with the engine mathematical model has shown that the helicopter will be able to perform both continued and rejected takeoffs if one engine fails at the CDP within quite a wide range of temperatures and altitudes.

Figs. 14 and 15 show time histories of the main helicopter motion parameters during continued takeoff (Fig. 14) and rejected takeoff (Fig. 15) from the CDP for normal takeoff weight of 14,200 kgf at an altitude of 500 m and ISA + 5 deg.C.

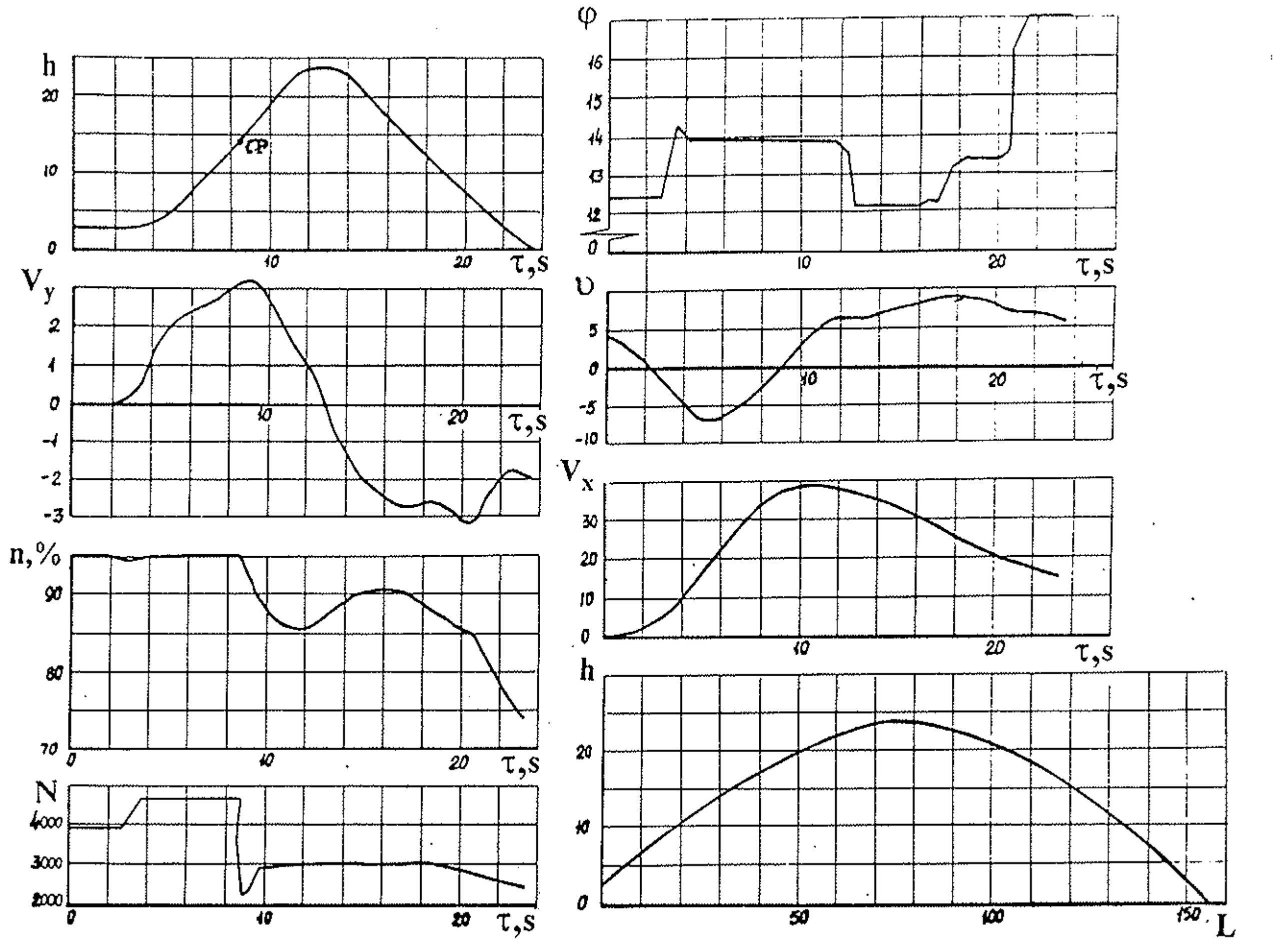

Fig.15. Helicopter motion main parameters variation in OEI rejected take-off from the critical point (H=500m, ISA+5°,M=14200kg)

And Fig. 16 presents the results of simulated continued takeoff from a site elevated relative to the surrounding surface, such as an off-shore oil rig platform. It can be seen that the helicopter can perform continued takeoff when one engine fails at the CDP at a height of 10 m; in this case it meets the FAR Part 29 requirements concerning the clearance to the rig structure and flight at an altitude not lower than 15 m above the surrounding surface.

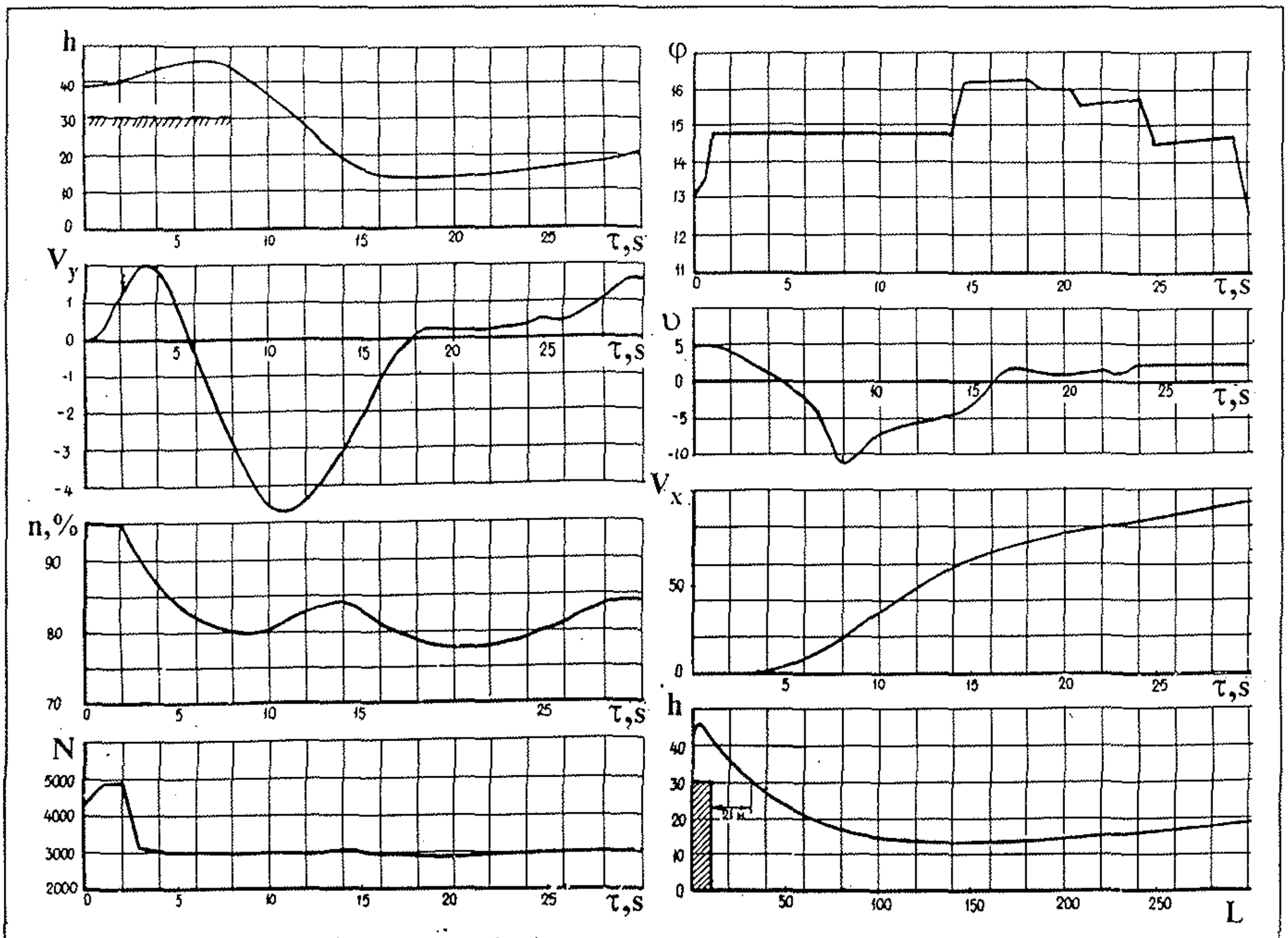

Fig.16. Time histories of main parameters for continued take-off when one engine fails above elevated site of limited size.(H=500m, ISA+5°,M=14200kg)

REFERENCES

1. A. Akimov and E. Vozhdaev "Flight research on Reducing Helicopter Parasite Drag". Paper No.-C21, Proceedings, 19th European Rotorcraft Forum, Cernobbio (Como), 1993.